The tunable VUV single-photon ionization mass spectrometry for the analysis of individual components in gasoline

Jing Wang [a], Bin Yang [a], Yuyang Li [a], Zhenyu Tian [a], Taichang Zhang [a], Fei Qi [a,*], Koichi Nakajima [b]

[a] *National Synchrotron Radiation Laboratory, University of Science and Technology of China, Hefei 230029, PR China*
[b] *Department of Chemistry, Science Research Center, Hosei University, Tokyo 102-8160, Japan*

Abstract

A procedure combining tunable vacuum ultraviolet (VUV) single-photon ionization with reflectron time-of-flight mass spectrometer has been developed for analysis of individual components in 90# unblended gasoline. Synchrotron radiation used as the ionization source can provide wide energy range and high resolution. All components can be identified by the molecular weights from photoionization mass spectrometry near threshold ionization and the ionization energies from photoionization efficiency spectra. About ninety components are detected in this study, including paraffins, olefins, and aromatics. Quantitative analysis can be obtained by the integrated ion intensity combining with data of photoionization cross-section. It appears that the tunable VUV photoionization mass spectrometry is a complementary method to previous existing ones for the analysis of individual components in gasoline. It may also be useful in other analytical applications.
© 2006 Elsevier B.V. All rights reserved.

Keywords: Components of gasoline; Tunable VUV photoionization; Time-of-flight mass spectrometry

1. Introduction

Gasoline is a complex mixture and contains hundreds of compounds including three major hydrocarbon types of paraffins, olefins, and aromatics. There is an increasing demand for analyzing or identifying individual components of gasoline in order to evaluate gasoline quality, meet regulatory requirements, guide refining processes, and blend oxygenates into final products, etc. A number of methods have been used for the analysis of hydrocarbon types such as paraffins, olefins, naphthenes, and aromatics (PONA). These methods include fluorescent indicator adsorption (FIA) [1], infrared (IR)/Fourier-transform infrared (FTIR) spectroscopy [2–4], nuclear magnetic resonance (NMR) spectroscopy [5–7], mass spectrometry (MS) [8], gas chromatography (GC) and GC combining with MS (GC/MS) [9–11]. However, these methods are normally used to determine one to several types of hydrocarbons in gasoline, although some of them can do so for several individual components.

The FIA method has long been used for the determination of hydrocarbons [1]. This method is simple and inexpensive; however, large amounts of conjugated diolefins in gasoline lead to ill-defined boundaries in the adsorption column, which make the reproducibility worse. On the other hand, IR and FTIR are spectroscopic techniques that do not require separation of individual components for determination of gasoline as well as that of oxygenates in gasoline [2–4]. Moreover, ^1H, ^{13}C or ^{17}O NMR spectroscopy has been devised for analysis of gasoline and oxygenates in gasoline by different research groups [5–7]. The NMR method is successful for determining oxygenates in the blended gasoline and providing PONA types. Compound types in gasoline have been analyzed by mass spectrometer previously [8]. The conventional ionization method used for MS is the electron-impact (EI) ionization with electron energy of 70 eV, which produces massive fragments. Thus it is often hard to interpret the EI mass spectrum due to overlaps of a large number of peaks including parent and fragment ion signals, although some components can be deduced from these specific fragment ions. GC and GC/MS are the most common methods in the petroleum industry all over the world, and are frequently used for the analysis and characterization of hydrocarbon-types in gasoline [9–11].

---

* Corresponding author. Tel.: +86 551 3602125; fax: +86 551 5141078.
  E-mail address: fqi@ustc.edu.cn (F. Qi).

More recently, mass spectrometry combined with the vacuum ultraviolet (VUV) single-photon ionization (SPI) or resonance-enhanced multiphoton ionization (REMPI) technique has been applied for the analysis of complex systems [12–17]. The laser-based REMPI technique is suitable for the selective and soft ionization with minimal fragmentation of aromatic compounds in complex mixtures, but not for the aliphatic compounds [12,14,15]. The VUV SPI method has been proven to be a promising method for determination of complex mixtures [12–17]. The VUV SPI technique is also a soft ionization method, which gives a single identifiable peak for each compound. However, a peak in mass spectrum could correspond to different isomers. There are many possible isomers for each mass, and the total number of possible isomers increases rapidly with increasing molecular weight. In principle, all isomers of each compound can be ionized once their ionization energies (IEs) are lower than the photon energy. Hence, determination of individual components only by molecular weights is less selective. The common light sources employed for the VUV SPI technique are light produced from laser frequency tripling in xenon with the wavelength of 118 nm or from the electron beam pumped VUV lamp or discharge lamp [12–17]. Mühlberger et al. used the VUV SPI technique for diverse applications [12–15,17]. Kuribayashi et al. used 121.6 nm VUV lamp to monitor chlorinated organic compounds in waste incineration flue gas [16]. The wavelength of the VUV lamps can be changed by filling different gases; the emitted wavelengths and bandwidth have been discussed in detail previously [12,17]. However, the wavelength from the lamps is not continuous at the VUV region. The synchrotron radiation has several advantages of continuous tunability, high energy resolution and high intensity at the VUV range. Very recently, Mysak et al. analyzed organic compounds in ultrafine and large aerosol particles with synchrotron based aerosol time-of-flight mass spectrometer [18].

In this paper, we analyze individual components of gasoline with the tunable VUV single-photon ionization. The study utilizes the tunable VUV light from synchrotron radiation combined with a reflectron time-of-flight MS (TOF MS). With the tunability of the VUV light, this method is thus universal and selective for analysis of complex systems including gasoline.

2. Experimental methods

Synchrotron radiation from a bend magnet of the 800 MeV electron storage ring of National Synchrotron Radiation Laboratory (NSRL) in Hefei, China, is monochromized with a 1 m Seya-Namioka monochromator equipped with two gratings (2400 and 1200 grooves/mm). The wavelength of the monochromator was calibrated with the known ionization energies of the inert gases. The energy resolution ($E/\Delta E$) is about 500–1000 depending on widths of slits. A 150 μm width was normally used for this study with the energy resolution of $\sim$500. The average photon flux was measured to be 5×10^{10} photons/s. A silicon photodiode (SXUV-100, International Radiation Detectors, Inc., USA) was used to monitor the photon flux for normalizing ion signals. Normally we use the 1200 grooves/mm grating with the wavelength range of 70–200 nm, which is sufficient to cover the IEs of all components in gasoline. A LiF window with 1.0 mm thickness was used to eliminate higher order radiation of the dispersed light in the wavelength region longer than 105 nm.

A schematic diagram of the experimental instrument is shown in Fig. 1. Briefly, the instrument consists of a sample inlet system, a differentially pumped chamber with molecular-beam sampling
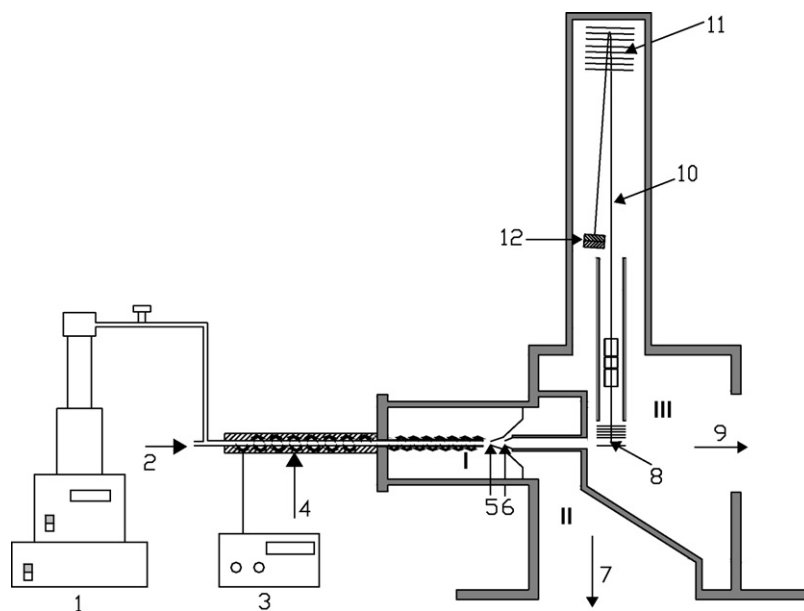

Fig. 1. Schematic diagram of the instrument including the sample inlet system (**I**), the differential pumped system (**II**), and the SPI chamber with the reflectron TOF MS (**III**). The other components include: (1) the syringe pump; (2) the carrier helium inlet; (3) the temperature controller; (4) the vaporizer; (5) the quartz nozzle with an orifice of 500 μm at the tip; (6) the nickel skimmer; (7) to a turbo molecular pump with the pump speed of 3500 l/s; (8) the ionization region; (9) to a turbo molecular pump with the pump speed of 1200 l/s; (10) the ion trajectory; (11) the ion optics of the reflectron; (12) the MCP detector.

Table 1
Gasoline specifications

Density (kg l^{-1})	0.737
10 vol.% evaporated boiling point (°C)	59
50 vol.% evaporated boiling point (°C)	105
90 vol.% evaporated boiling point (°C)	159
Final boiling point (°C)	184
Compositions (vol.%)	
Paraffins	47
Olefins	29
Aromatics	24

Note: The 90# standard unblended gasoline for this experiment was provided by Fangyuan Inc., Liaoning, China. Data of the specifications are provided by the vendor.

system, and a photoionization chamber with a reflectron TOF MS for ion detection.

The 90# standard unblended gasoline for this experiment was provided by Fangyuan Inc., Liaoning, China. The specifications of gasoline are listed in Table 1. A syringe pump (ISCO, Inc., USA) was used to control the flow rate of gasoline. The gasoline with the carrier gas (helium) was vaporized and entered into the sample inlet chamber (part **I** in Fig. 1) through a quartz tube with an inner diameter of 5.0 mm, which was also heated. The temperature of the vaporizer and the quartz tube was maintained at 200 °C to ensure that the gasoline was vaporized completely. The flow rate of liquid gasoline was 0.100 ml/min at room temperature, and the flow rate of He was 0.600 standard liters per minute (SLM) controlled by the MKS mass flow controller. Then gas-phase mixture of gasoline and He was sampled through a quartz cone-like nozzle with an orifice of ∼500 μm in diameter. A nickel skimmer with a 2 mm diameter aperture was located 18 mm downstream from the sampling nozzle. The sample gases formed a molecular beam, which passed horizontally through the 10 mm gap between the repeller and extractor plates of reflectron TOF MS. The molecular beam intersected perpendicularly with synchrotron VUV light beam. The sample inlet chamber (**I**) was pumped with a 27 l/s mechanical pump and a 70 l/s roots pump. The differentially pumping chamber (**II**) was pumped with a 3500 l/s turbo molecular pump, which was backed by a 15 l/s mechanical pump plus a 70 l/s roots pump. The photoionization chamber (**III**) was pumped with a 1200 l/s turbo molecular pump and a 15 l/s mechanical pump. The pressures in the sample inlet chamber, the differentially pumped chamber and the ionization chamber were 400, 3.3×10^{-3}, and 1.1×10^{-3} Pa, respectively.

The ion signal was detected with the reflectron TOF MS, which was installed in the photoionization chamber vertically (see Fig. 1). A detail description on the ion optics of the reflectron TOF MS has been published elsewhere [19,20], and it is briefly outlined here. A pulsed voltage of 385 V was used to propel ions into the flight tube, and finally to a microchannel plate (MCP) detector. The total flight length of the ions was 1.8 m. The ion signals were amplified by a pre-amplifier (VT120C, EG&G ORTEC, USA). The mass resolution ($m/\Delta m$) was measured to be ∼1400. A digital delay generator (DG535, Stanford Research System, USA) was used to trigger the pulse power supply and to feed as the start of a multiscaler with repetition ratio of 18 kHz.

The multiscaler (FAST Comtec P7888, Germany) was used to record signals of mass spectrum with 2 ns bin width. A small bias voltage (1.0 V) was added to the extraction plate to improve signal intensity, reduce the background ions, and enhance the mass resolution [19].

3. Results and discussion

3.1. Characterization of the instrument

The proposed procedure was tested with a mixture of three compounds including 1 ml *p*-xylene, 3 ml ethylbenzene and 6 ml benzaldehyde, which have the close molecular weights of 106 Da. The flow rates of the liquid mixture and helium were 0.100 ml/min and 0.650 SLM controlled by the syringe pump and the MKS mass flow controller, respectively.

Fig. 2 shows a photoionization mass spectrum (PIMS) of the mixture measured at the photon energy of 9.18 eV (135.0 nm) in 30 s. Only one strong peak is observed at $m/z = 106$ and the weak peak at $m/z = 107$ is attributed to ^{13}C isotope contribution, which indicates that these isomers can hardly be distinguished from a single mass spectrum. There are many isomeric components with close molecular weights in gasoline. Hence, isomeric identification is a crucial step for analysis of individual components in gasoline, especially for those large molecules which were difficult to be identified in previous studies. In this work, the photon energy can be selected in order to ensure the near threshold VUV SPI. Hence no fragment ions can be formed at the selected photon energy. With the tunability of the light source, we can measure a series of mass spectra at different wavelengths. Then each mass peak is integrated to yield the photoionization efficiency (PIE) spectra, a plot of ion intensity vs. photon energy. The value of IE can be obtained from the PIE spectra directly. Considering energy resolution of the monochromator and the cooling effect of molecular beam [21], the experimental error of determined IEs is within 0.05 eV. The isomers can be determined by comparing the experimental IEs with known literature values.
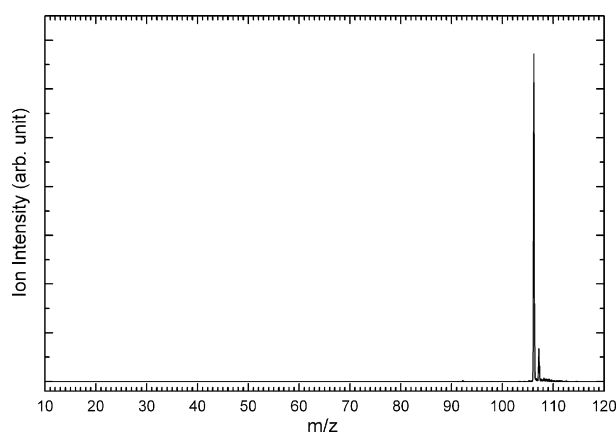

Fig. 2. VUV single-photon ionization mass spectrum of the mixture including *p*-xylene, ethylbenzene and benzaldehyde at the photon energy of 9.18 eV (135.0 nm). The measurement time is 30 s.
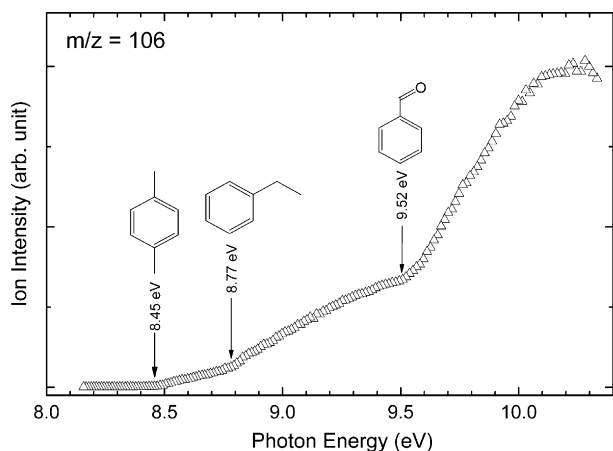
Fig. 3. The PIE spectra of $m/z = 106$ sampled from the mixture including *p*-xylene, ethylbenzene and benzaldehyde. Three observed onsets at 8.45, 8.77, and 9.52 eV correspond to the IEs of *p*-xylene, ethylbenzene and benzaldehyde, respectively.

The PIE spectra of the mixture is shown in Fig. 3. Three onsets are clearly observed at 8.45, 8.77, and 9.52 ± 0.05 eV. They correspond to the IEs of *p*-xylene, ethylbenzene and benzaldehyde, which have the literature values of 8.44, 8.77, and 9.50 eV, respectively [22]. We have thus confirmed that the liquid sample consists of the three components: *p*-xylene, ethylbenzene and benzaldehyde. It should be pointed out that this method is unable to distinguish the molecules with the same molecular weight as well as similar IEs.

3.2. Individual componential analysis in gasoline

Fig. 4 shows four VUV PIMS of the standard 90# gasoline at the photon energies of 10.78 eV (115.0 nm), 9.92 eV (125.0 nm), 9.18 eV (135.0 nm) and 8.55 eV (145.0 nm), respectively. The measurement time for each mass spectrum is 30 s. A large number of peaks at the mass range of 42–170 are observed in the PIMS at the photon energy of 10.78 eV, which correspond to hydrocarbons ranging from C_4 to C_{13}. However, not all peaks are formed from components of gasoline. The peaks with the odd m/z are mostly produced from the fragmentation of large hydrocarbons, as the photon energy is high enough to produce fragmentation. Therefore, these peaks with the odd molecular weight disappear gradually, while the photon energy decreases and becomes lower than the appearance potentials (AP) of the corresponding fragment ions. On the other hand, the peaks with the even m/z at the photon energy of 10.78 eV correspond to components in the gasoline except for the mass 42 (C_3H_6). The measurement of the PIE spectra of mass 42 shows an onset at 10.12 eV which are much higher than the IE of propylene is 9.73 eV [22]. Thus we can conclude that C_3H_6 is not the component of gasoline; it is formed from fragmentation of larger hydrocarbons at the 10.78 eV.

The PIE spectra of all observed peaks from gasoline were measured with the photon energy ranging from 7.8 to 10.5 eV. The baseline has been subtracted from the integrated ion intensity. Here we choose several PIE spectra to illustrate how to identify the isomers, as shown in Fig. 5. The PIE spectra of
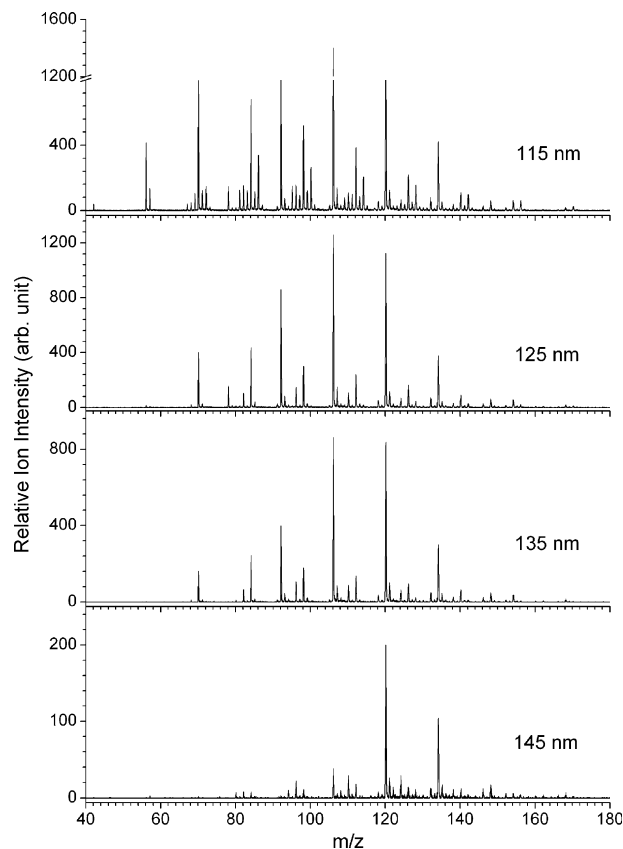

Fig. 4. Four VUV photoionization mass spectra of gasoline at the photon energies of 10.78 eV (115.0 nm), 9.92 eV (125.0 nm), 9.18 eV (135.0 nm) and 8.55 eV (145.0 nm), respectively.

$m/z = 84$ is shown in Fig. 5(a). Three onsets are observed at 8.27, 8.58, and 8.97 ± 0.05 eV, which correspond to the IEs of 2,3-dimethyl-2-butene (IE = 8.27 eV [22]), 2(3)-methyl-2-pentene (IE = 8.58 eV [22]) and 2(3)-hexene or 4-methyl-2-pentene (IE = 8.95 eV for 3-hexene [22], IE = 8.97 eV for 2-hexene [22], IE = 8.98 eV for 4-methyl-2-pentene [22]), respectively. It's hard to distinguish 2-hexene, 3-hexene and 4-methyl-2-pentene, since the IEs of these three isomers are close to each other. Similarly, 2-methyl-2-pentene and 3-methyl-2-pentene cannot be identified by their IEs, too. A relatively strong peak is observed for mass 92 in Fig. 4 at the photon energies of 10.78, 9.82, and 9.18 eV. Fig. 5(b) shows the PIE spectra of mass 92. An apparent onset at 8.82 eV corresponds to the IE of toluene. Based on the measurement of the PIE spectra in Fig. 5(c), at least three onsets can be observed for $m/z = 112$: 8.48, 8.90, and 9.76 ± 0.05 eV. The onsets at 8.48 and 9.76 eV are attributed to the ionization of 3-ethyl-3-hexene (IE = 8.48 eV [22]) and cyclooctane (IE = 9.75 eV [22]), respectively. Besides, the threshold at 8.90 eV is close to the IEs of three isomers: 2,4,4-trimethyl-1-pentene (IE = 8.909 eV [22]), 2-octene (IE = 8.913 eV [22]), and 4-octene (IE = 8.913 eV [22]). The PIE spectra of $m/z = 128$, shown in Fig. 5(d), have two apparent onsets at 8.18 and 9.71 ± 0.05 eV, which correspond to an aromatic hydrocarbon, naphthalene (IE = 8.144 eV [22]) and a paraffin, nonane (IE = 9.71 eV [22]), respectively. The measured ionization thresholds for all observed peaks are listed in Table 2,
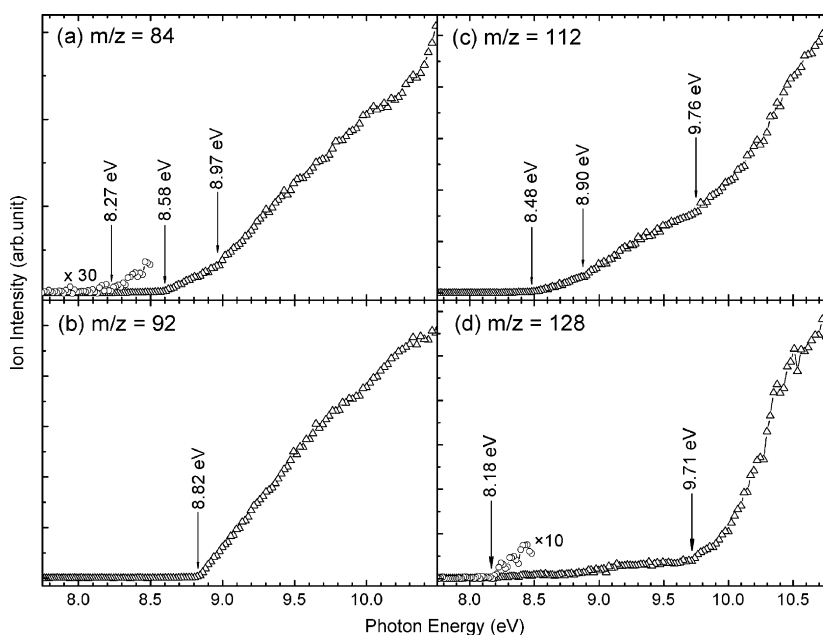
Fig. 5. The PIE spectra of (a) $m/z = 84$ (C_6H_{12}), (b) $m/z = 92$ (C_7H_8), (c) $m/z = 112$ (C_8H_{16}), and (d) $m/z = 128$ ($C_9H_{20}/C_{10}H_8$) sampled from gasoline.

along with the IEs from the literature. Many hydrocarbons are identified, including paraffins (isoparaffins), naphthenes, olefins, diolefins, cyclo-olefins, cyclo-diolefins, and aromatics, as seen in Table 2.

The ion signal intensity of the mass spectrum is proportional to the concentration of species and its specific photoionization cross-section, as indicated by the following equation [23]:

$$I_i = \rho_i \sigma_i(E)C.$$

Here I_i is the integrated ion intensity of species i, ρ_i is the concentration of species i, $\sigma_i(E)$ is the photoionization cross-section of the species i at the photon energy E, and C is a constant for the instrument. Absolute photoionization cross-sections for some hydrocarbons can be found from the literatures [24]. However, the photoionization cross-sections of species with large molecular weights are insufficient and hard to obtain experimentally. Nevertheless reasonable estimations for absolute photoionization cross-sections can be made based on known cross-sections for molecules with similar functional groups. To the end, the number of C=C double, C≡C triple bonds, the different ionization energies, and the photon energies used for the concentration determinations are taken into account. The estimation of the photoionization cross-sections is based on the parent ions. At the photon energy of 10.78 eV, all components in gasoline can be ionized. The average photoionization cross-sections are estimated to be 4 and 22 Mb for paraffins and olefins, respectively, according to an empirical equation proposed by Koizumi [25]. The simplest aromatics is benzene; its photoionization cross-section is 32 Mb at 10.78 eV [24]. Generally, the IEs of aromatics decrease with the increasing molecular weights; thus an estimated photoionization cross-section of 35 Mb at 10.78 eV is used for calculating concentrations of aromatics. Therefore, the concentrations of these large components in gasoline are deduced from their integrated ion

intensities at mass spectrum combining with estimated average photoionization cross-sections. This simplification can give an acceptable quantitative analysis by choosing a mass spectrum at the suitable photon energy. Here we calculate the concentrations using the mass spectrum at the photon energy of 10.78 eV.

In this work, we have not considered the fragmentation of hydrocarbons in gasoline at 10.78 eV. All even mass peaks are integrated, which are determined to be the components in gasoline by IE measurements; the calculated concentration for each mass is listed in Table 2 as well. The relative concentration for each mass in Table 2 includes contributions from all isomers for this mass. For example, the relative concentration of mass 56 (C_4H_8) is 1.04% as shown in Table 2, which includes the contributions from three isomers: 2-methyl-1-propene, 1-butene, and cyclobutane. The lowest relative concentration is found to be 0.01% for $C_{12}H_{16}$ (cyclohexylbenzene) and $C_{13}H_{10}$ (fluorene). The heaviest hydrocarbon identified in the gasoline is _n_-dodecane in this study. According to the data in Table 2, the paraffins are the dominant components in the gasoline. For example, the relative concentrations of C_4H_{10}, C_5H_{12}, C_6H_{14}, C_7H_{16}, C_8H_{18}, C_9H_{20}, $C_{10}H_{22}$, $C_{11}H_{24}$, and $C_{12}H_{26}$ are calculated to be 0.10, 4.80, 11.10, 10.40, 8.70, 6.87, 3.95, 2.16, and 0.84%, respectively. Unsaturated aliphatic hydrocarbons are abundant in the gasoline, especially olefins, such as C_4H_8 (1.04%), C_5H_{10} (4.96%), C_6H_{12} (4.81%), C_7H_{14} (3.79%), C_8H_{16} (2.80%), C_9H_{18} (1.72%), and $C_{10}H_{20}$ (0.85%). Furthermore, the relative concentrations of the aromatics are obtained to be 0.73% for C_6H_6, 3.91% for C_7H_8, 6.97% for C_8H_{10}, 5.57% for C_9H_{12}, 1.86% for $C_{10}H_{14}$, 0.27% for $C_{11}H_{16}$, and 0.03% for $C_{12}H_{18}$. The relative concentrations of paraffins, olefins, and aromatics are calculated to be 48.9, 29.4, and 21.7%, respectively, in agreement with the specifications provided by the vendor, as shown in Table 1. The difference between the two sets

Table 2
Components in the gasoline 90# with their IEs measured from this work and from the literature, and relative concentrations

m/z	Formula	IE (eV)		Species	Relative concentration (%)[a]
		This work (±0.05 eV)	Literature [22]		
56	C_4H_8	9.22	9.22	2-Methyl-1-propene	1.04
		9.51	9.55	1-Butene	
		9.83	9.80	Cyclobutane	
58	C_4H_{10}	10.52	10.53	Butane	0.10
68	C_5H_8	8.60	8.59	1,3-Pentadiene	0.34
		8.86	8.86	2-Methyl-1,3-butadiene	
		9.02	9.01	Cyclopentene	
70	C_5H_{10}	8.68	8.69	2-Methyl-2-butene	4.96
		9.02	9.01	2-Pentene	
		10.34	10.33	Cyclopentane	
72	C_5H_{12}	10.27	10.28	Pentane	4.80
78	C_6H_6	9.24	9.24	Benzene	0.73
80	C_6H_8	8.24	8.25	1,3-Cyclohexadiene	0.09
82	C_6H_{10}	8.57	8.55	1-Methyl-1-cyclopentene	1.02
84	C_6H_{12}	8.27	8.27	2,3-Dimethyl-2-butene	4.81
		8.58	8.58	2-Methyl-2-pentene	
			8.58	3-Methyl-2-pentene	
		8.97	8.95	3-Hexene	
			8.97	2-Hexene	
			8.98	4-Methyl-2-pentene	
86	C_6H_{14}	10.02	10.02	2,3-Dimethylbutane	11.10
		10.22	10.13	Hexane	
92	C_7H_8	8.82	8.83	Toluene	3.91
94	C_7H_{10}	7.92	7.96	(E,E)-1,3,5-Heptatriene	0.15
96	C_7H_{12}	8.18	8.17	2,4-Heptadiene	1.10
			8.19	4-Methyl-(E)-1,3-hexadiene	
		8.53	8.53	1-Ethylcyclopentene	
98	C_7H_{14}	8.21	8.21	2,3-Dimethyl-2-pentene	3.79
		8.57	8.62	2-Methyl-2-hexene	
		9.38	9.34	1-Heptene	
		10.00	9.9	Cycloheptane	
			9.92	1,2-Dimethylcyclopentane	
100	C_7H_{16}	9.95	9.93	Heptane	10.40
106	C_8H_{10}	8.44	8.44	p-Xylene	6.97
		8.57	8.55	m-Xylene	
			8.56	o-Xylene	
		8.78	8.77	Ethylbenzene	
110	C_8H_{14}	8.13	8.13	2,4-Octadiene	0.66
		8.48	8.47	Ethylidenecyclohexane	
			8.48	1-Ethylcyclohexene	
			8.48	1-Propylcyclopentene	
112	C_8H_{16}	8.48	8.48	3-Ethyl-3-hexene	2.80
		8.90	8.91	2,4,4-Trimethyl-1-pentene	
			8.91	2-Octene	
			8.91	4-Octene	
		9.76	9.75	Cyclooctane	
114	C_8H_{18}	9.87	9.80	Octane	8.70
			9.84	2-Methylheptane	
			9.89	Isooctane	
118	C_9H_{10}	8.46	8.46	Indane	0.22
120	C_9H_{12}	8.27	8.27	1,2,4-Trimethylbenzene	5.57
		8.48	8.48	1,2,3-Trimethylbenzene	

Table 2 (*Continued*)

m/z	Formula	IE (eV)		Species	Relative concentration (%)[a]
		This work (±0.05 eV)	Literature [22]		
124	C_9H_{16}	8.46	8.43	1-Propylcyclohexene	0.50
			8.44	1-Isobutyl-1-cyclopentene	
			8.45	1-Butylcyclopentene	
			8.44	(*E*)-1,3-Nonadiene	
126	C_9H_{18}	8.82	8.80	4-Nonene	1.72
			8.84	3-Nonene	
		9.40	9.38	1,2,4-Trimethylcyclohexane	
			9.39	1,1,3-Trimethylcyclohexane	
			9.42	1-Nonene	
		9.96	9.95	Butylcyclopentane	
128	$C_{10}H_8$	8.18	8.14	Naphthalene	6.87
	C_9H_{20}	9.71	9.71	Nonane	
132	$C_{10}H_{12}$	8.23	8.22	2,4-Dimethylstyrene	0.45
		8.47	8.46	Tetralin	
			8.48	(*E*)-1-Phenyl-2-butene	
134	$C_{10}H_{14}$	8.06	8.06	1,2,4,5-Tetramethylbenzene	1.86
		8.43	8.47	1,2,3,5-Tetramethylbenzene	
136	$C_{10}H_{16}$	8.07	8.07	α-Pinene	4.92
		8.40	8.4	3-Carene	
138	$C_{10}H_{18}$	8.81	8.80	3-Butylcyclohexene	0.19
			8.83	1-Isopentyl-1-cyclopentene	
140	$C_{10}H_{20}$	8.25	8.24	2,3,4,5-Tetramethyl-3-hexene	0.85
		8.76	8.762	5-Decene	
			8.78	4-Decene	
		9.41	9.42	1-Decene	
142	$C_{10}H_{22}$	9.65	9.65	Decane	3.95
	$C_{11}H_{10}$	7.96	7.96	1-Methylnaphthalene	
			7.91	2-Methylnaphthalene	
146	$C_{11}H_{14}$	8.00	7.9	Cyclopentylbenzene	1.77
			8.1	(1-Methylcyclobutyl)-benzene	
148	$C_{11}H_{16}$	8.09	8.12	4-*tert*-Butyltoluene	0.27
		8.41	8.4	1-Methyl-3-butylbenzene	
			8.4	1-Methyl-4-butylbenzene	
			8.41	2,2-Dimethyl-1-phenylpropane	
152	$C_{12}H_8$	8.11	8.12	Acenaphthylene	0.06
154	$C_{12}H_{10}$	8.30	8.16	Biphenyl	0.23
156	$C_{12}H_{12}$	7.92	7.89	2,3-Dimethylnaphthalene	2.16
			7.89	2,7-Dimethylnaphthalene	
			7.95	2-Ethylnaphthalene	
	$C_{11}H_{24}$	9.60	9.56	Undecane	
160	$C_{12}H_{16}$	8.11	8.1	Cyclohexylbenzene	0.01
162	$C_{12}H_{18}$	8.32	8.32	1,3,5-Triethylbenzene	0.03
			8.31	1,4-Dipropylbenzene	
166	$C_{13}H_{10}$	8.05	7.91	Fluorene	0.01
168	$C_{13}H_{12}$	8.12	8.10	2-Methyl-1,1′-biphenyl	0.05
		8.53	8.55	Diphenylmethane	
170	$C_{12}H_{26}$	9.60	9.59[b]	*n*-Dodecane	0.84

[a] *Note*: The values are the total relative concentration of a specific mass. For example, the relative concentration of 1.04% for mass 56 includes 2-methyl-1-propene, 1-butene and cyclobutane.

[b] No experimental IE value is found for *n*-dodecane. This IE is from the energy difference between neutral $C_{12}H_{26}$ and cation $C_{12}H_{26}^+$ calculated at the B3LYP/6-311++ *G*(2d,p) level.

of results is mainly due to the uncertainty of the photoionization cross-sections.

The method proposed in this work provides qualitative and quantitative information for individual hydrocarbons in the gasoline, which is a good complementary one for existing methods. Currently, the only disadvantage is the need for access to a synchrotron radiation facility. As more and more synchrotron facilities and VUV free electron lasers become available, the tunable VUV single-photon ionization in combination with established methods (for example, GC) will be greatly helpful in various analytical fields.

4. Conclusions

The procedure combining tunable VUV SPI with reflectron TOF MS provides a novel and selective method for the analysis of individual components in the gasoline. The tunable VUV SPI can minimize fragmentation due to the near-threshold photoionization. Since synchrotron light is tunable and has good energy resolution at the VUV range, it is suitable for the determination of individual species in gasoline by measurements of the PIMS and PIE spectra. The quantitative analysis is obtained with data of the photoionization cross-sections. The lowest relative concentration is measured to be 0.01%. It can also be applied to the analysis of components in many other samples or situations, such as mobile engine exhaust, cigarette smoke, pyrolysis of coal, biomass, and polymers, etc.

Acknowledgments

References

[1] A.L. Conrad, Anal. Chem. 20 (1948) 725.
[2] S.E. Fry, M.P. Fuller, F.T. White, D.R. Battlste, Anal. Chem. 55 (1983) 407.
[3] G.E. Fordor, K.B. Kohl, R.L. Mason, Anal. Chem. 68 (1996) 23.
[4] A. Lob, R. Buenafe, N.M. Abbas, Fuel 77 (1998) 1861.
[5] R. Meusinger, Fuel 75 (1996) 1235.
[6] A.S. Sarpal, G.S. Kapur, S. Mukherjee, S.K. Jain, Energy Fuels 11 (1997) 662.
[7] D.G. Lonnon, J.M. Hook, Anal. Chem. 75 (2003) 4659.
[8] R.A. Brown, Anal. Chem. 23 (1951) 430.
[9] H.S. Knight, Anal. Chem. 30 (1958) 9.
[10] P. Doble, M. Sandercock, E.D. Pasquier, P. Petocz, C. Roux, M. Dawson, Forensic Sci. Int. 132 (2003) 26.
[11] F. Mühlberger, T. Streibel, J. Wieser, A. Ulrich, R. Zimmermann, Anal. Chem. 77 (2005) 7408.
[12] F. Mühlberger, R. Zimmermann, A. Kettrup, Anal. Chem. 73 (2001) 3590.
[13] F. Mühlberger, J. Wieser, A. Ulrich, R. Zimmermann, Anal. Chem. 74 (2002) 3790.
[14] L. Cao, F. Mühlberger, T. Adam, T. Streibel, H.Z. Wang, A. Kettrup, R. Zimmermann, Anal. Chem. 75 (2003) 5639.
[15] F. Mühlberger, K. Hafner, S. Kaesdorf, T. Ferge, R. Zimmermann, Anal. Chem. 76 (2004) 6753.
[16] S. Kuribayashi, H. Yamakoshi, M. Danno, S. Sakai, S. Tsuruga, H. Futami, S. Morii, Anal. Chem. 77 (2005) 1007.
[17] F. Mühlberger, J. Wieser, A. Morozov, A. Ulrich, R. Zimmermann, Anal. Chem. 77 (2005) 2218.
[18] E.R. Mysak, K.R. Wilson, M. Jimenez-Cruz, M. Ahmed, T. Baer, Anal. Chem. 77 (2005) 5953.
[19] C.Q. Huang, B. Yang, R. Yang, J. Wang, L.X. Wei, X.B. Shan, L.S. Sheng, Y.W. Zhang, F. Qi, Rev. Sci. Instrum. 76 (2005) 126108.
[20] F. Qi, R. Yang, B. Yang, C.Q. Huang, L.X. Wei, J. Wang, L.S. Sheng, Y.W. Zhang, Rev. Sci. Instrum. 77 (2006) 084101.
[21] M. Kamphus, N.-N. Liu, B. Atakan, F. Qi, A. Mcllroy, Proc. Combust. Inst. 29 (2002) 2627.
[22] P.J. Linstrom, W.G. Mallard, NIST Chemistry Webbook, NIST Standard Reference Database Number 69, Gaithersburg, MD, 2003.
[23] T.A. Cool, K. Nakajima, C.A. Taatjes, A. McIlroy, P.R. Westmoreland, M.E. Law, A. Morel, Proc. Combust. Inst. 30 (2005) 1681.
[24] T.A. Cool, J. Wang, K. Nakajima, C.A. Taatjes, A. Mcllroy, Int. J. Mass. Spectrom. 247 (2005) 18.
[25] H. Koizumi, J. Chem. Phys. 95 (1991) 5846.